The Sec63/BiP complex suppresses higher-order oligomerization and RNase activity of IRE1α during ER stress

Xia Li[1], Sha Sun[1], Suhila Appathurai[1], Arunkumar Sundaram[1], Rachel Plumb[1], and Malaiyalam Mariappan[*]

Department of Cell Biology
Nanobiology Institute
Yale School of Medicine
Yale West Campus
West Haven, CT 06516, USA

[*] Correspondence: malaiyalam.mariappan@yale.edu

Abstract: IRE1α is a conserved branch of the unfolded protein response (UPR) that detects unfolded proteins in the lumen of the endoplasmic reticulum (ER) and propagates the signal to the cytosol. We have previously shown that IRE1α forms a complex with the Sec61 translocon to cleave its substrate mRNAs (Plumb et al., 2015). This complex also regulates IRE1α activation dynamics during ER stress in cells (Sundaram et al., 2017), but the underlying mechanism is unclear. Here, we show that Sec63 is a subunit of the IRE1α/Sec61 translocon complex. Sec63 recruits and activates BiP ATPase through its luminal J-domain to bind onto IRE1α. This Sec63-mediated BiP binding to IRE1α suppresses the formation of higher-order oligomers of IRE1α, leading to proper attenuation of IRE1α RNase activity during persistent ER stress. Thus, our data suggest that the Sec61 translocon bridges IRE1α with Sec63/BiP to regulate the dynamics of IRE1α activity in cells.

Introduction

Secretory and membrane proteins are initially synthesized and folded in the endoplasmic reticulum (ER). The majority of these nascent proteins are delivered to the Sec61 translocon in the ER membrane by the co-translational protein targeting pathway (Rapoport, 2007, Shao and Hegde, 2011). The Sec61 translocon facilitates the translocation and insertion of newly synthesized secretory and membrane proteins. Immediately after entering the ER, they are folded and assembled with the help of glycosylation, chaperones, and folding enzymes in the ER (van Anken 2005). However, the ER capacity to fold newly synthesized proteins is often challenged by several conditions, including a sudden increase in incoming protein load, expression of aberrant proteins, and environmental stress. Under such conditions, terminally misfolded and unassembled proteins are recognized by the ER associated degradation (ERAD) pathway for the proteasomal degradation (Brodsky, 2012). When misfolded proteins overwhelm the ERAD capacity, they accumulate in the ER, thus causing ER stress, which in turn triggers a signaling network called the unfolded protein response (UPR) (Walter and Ron, 2011). The UPR restores the ER homeostasis by both reducing incoming protein load as well as increasing the protein folding capacity of the ER. If ER stress is unmitigated, the UPR has been shown to initiate apoptosis to eliminate non-functional cells (Hetz, 2012). The UPR-mediated life-and-death decision is implicated in several human diseases, including diabetes, cancer, and neurodegeneration (Wang and Kaufman, 2016).

Three major transmembrane ER stress sensor proteins are localized in the ER, namely IRE1α, PERK and ATF6 (Walter and Ron, 2011). IRE1α is a conserved transmembrane kinase/endonuclease, which is activated by self-oligomerization and trans-autophosphorylation during ER stress conditions (Cox et al., 1993; Mori et al., 1993). Once activated, IRE1α mediates nonconventional splicing of XBP1 mRNA (Yoshida et al., 2001; Calfon et al., 2002), which is recruited to the Sec61 translocon through its ribosome nascent chain (Yanagitani et al., 2011; Plumb et al., 2015; Kanda et al., 2016). Nearly all endogenous IRE1α molecules exist in a complex with the Sec61 translocon in cells (Plumb et al., 2015). The cleaved fragments of XBP1 mRNA are subsequently ligated by the RtcB tRNA ligase (Lu et al., 2014; Jurkin et al., 2014; Kosmaczewski et al., 2014) with its co-factor archease (Poothong et al., 2017). The spliced

XBP1 mRNA is translated into a functional transcription factor, which induces the expression of chaperones, quality control factors, and protein translocation components (Lee et al., 2003). IRE1α can also promiscuously cleave many ER-localized mRNAs through the regulated Ire1-dependent decay (RIDD) pathway, which is implicated in reducing the incoming protein load to the ER (Hollien and Weissman, 2006; Han et al., 2009). PERK is a transmembrane kinase and is responsible for phosphorylating the α subunit of eIF2 during ER stress, which causes global inhibition of translation in cells, thus alleviating the burden of protein misfolding in the ER (Harding et al., 1999; Sood et al., 2000). ATF6 is an ER-localized transcription factor and is translocated to Golgi upon ER stress where it is cleaved by intramembrane proteases (Haze et al., 1999; Ye et al., 2000). This causes the release of the cytosolic transcription domain into the cytosol and to the nucleus where it upregulates genes encoding ER chaperones and quality control factors to restore ER homeostasis (Lee et al., 2003; Shoulders et al., 2013).

The activity of all three UPR sensors are tightly regulated both under homeostatic and ER stress conditions, but the underlying mechanisms are poorly understood. In particular, it is important to understand the regulation of IRE1α activity since sustained activation of IRE1α is implicated in many human diseases including type 2 diabetes (Lin et al., 2007; Ghosh et al., 2014). On the other hand, hyperactivated IRE1α can produce excess of XBP1 transcription factor, which can be beneficial for tumor cell growth in a hostile environment (Cubillos-Ruiz et al., 2017). Recent studies have identified many IRE1α interacting proteins that have been shown to regulate IRE1α activation and inactivation during ER stress (Eletto et al., 2014; Sundaram et al., 2017; Sepulveda et al., 2018). One of the key factors that regulate IRE1α activity is the luminal Hsp70 like chaperone BiP ATPase (Bertolotti et al., 2000; Okamura et al., 2000; Pincus et al., 2010; Amin-Wetzel et al., 2017). IRE1α binding to BiP inhibits its oligomerization, thereby suppressing its RNase activity. However, it is unclear how the luminal protein BiP is efficiently recruited to the membrane-localized IRE1α in cells. Our previous studies have shown that IRE1α interaction with the Sec61 translocon is essential to regulate its oligomerization and RNase activity in cells (Sundaram et al., 2017). However, the molecular mechanism by which the Sec61 translocon limits IRE1α activity is unclear. In this study, we found that the Sec61 translocon bridges the interaction between IRE1α and Sec63. The J domain of Sec63 is responsible for recruiting and activating the luminal BiP ATPase to bind onto IRE1α, thus suppressing IRE1α higher order oligomerization and RNase activity.

Results

Sec61 translocon-mediates the interaction between IRE1α and Sec63

To determine the mechanism by which the Sec61 translocon limits IRE1α oligomerization and RNase activity, we looked back at our previous results on IRE1α interacting proteins (Plumb et al., 2015 and Sundaram et al., 2017). In addition to the Sec61 translocon, Sec63 is also enriched in the affinity purified IRE1α sample. Sec63 is a conserved translocon interacting membrane protein involved in protein translocation into the ER (Deshaies et al., 1991; Panzner et al., 1995; Meyer et al., 2000). While Sec63 is known to play a key role in the post-translational protein translocation into the ER, it can also assist the co-translational protein translocation into the ER (Brodsky et al., 1995; Young et al., 2001; Conti et al., 2015). We first

investigated whether IRE1α interacts with Sec63 through the Sec61 translocon. To test this, we immunoprecipitated several translocon interaction defective IRE1α mutants and looked for an association with Sec63 (Figure 1A). These IRE1α mutants showed a weak association with Sec63 as well, suggesting that IRE1α interacts with Sec63 via the Sec61 translocon (Figure 1A, B). Interestingly, IRE1α did not coimmunoprecipitate with Sec62, which is known to form a complex with Sec61/Sec63 (Panzner et al., 1995). In addition to the previously described luminal juxtamembrane region (Plumb et al., 2015), we identified that the transmembrane domain (TMD) of IRE1α also important for the interaction with Sec61/Sec63 since replacing IRE1α TMD with the TMD from calnexin abolished the interaction with the translocon complex (Figure 1A, B). We reasoned that if IRE1α interacts with Sec63 through the translocon, depletion of Sec63 would have less effect on the interaction between IRE1α and the translocon. To test this, we generated HEK293 Sec63-/- cells using CRISPR/Cas9. Immunoprecipitation of IRE1α from wild type cells revealed an interaction between IRE1α and the Sec61/Sec63 complex (Figure 1C). As expected, the translocon interaction defective mutant IRE1αΔ10 showed almost no association with Sec63. The knockout of Sec63 slightly reduced but did not abolish the interaction between IRE1α and Sec61, suggesting that IRE1α can interact with the translocon independent of Sec63 (Figure 1C). Again, IRE1α selectively interacted with a Sec61 translocon complex that contains Sec63, but not Sec62. This observation is further supported by the evidence that Sec63 mutants that poorly interacted with the Sec61 translocon also showed less interaction with the endogenous IRE1α (Figure 1D; Figure 1 - figure supplement 1). Sec61/Sec63 selectively interacted with the IRE1α branch of the UPR since they did not interact with either PERK or ATF6 (Figure 1D). We next asked whether the interaction between Sec63 and IRE1α is preserved during ER stress conditions to regulate IRE1α RNase activity. To test this, we immunoprecipitated Sec63 from Sec63-/- cells complemented with wild type Sec63-FLAG that were treated with or without ER stress inducers, thapsigargin (Tg), tunicamycin (Tm) or dithiothreitol (DTT) (Figure 1E). Sec63 interaction with the endogenous IRE1α was slightly disrupted upon treatment of the cells with Tg, TM, or DTT for 4h, suggesting that Sec63 may play an important role in regulating IRE1α activity during ER stress. However, a longer ER stress treatment with DTT (8h) severely disrupted the IRE1/Sec63/Sec61 complex (Figure 1E).

Sec63 suppresses the higher-order oligomerization of IRE1α

It is known that IRE1α forms higher-order oligomers or clusters in cells upon ER stress, which correlate with IRE1α RNase activity (Li et al., 2010). We have previously shown that IRE1α interaction with the Sec61 translocon is crucial for limiting IRE1α clusters in cells during ER stress conditions (Sundaram et al., 2017). We speculated that this activity was mainly due to the Sec61 translocon-associated Sec63, which can recruit BiP through its luminal J domain to suppress IRE1α higher-order oligomers. To test this idea, we performed siRNA mediated knockdown of Sec63 in cells and monitored IRE1α clustering by confocal immunofluorescence after treatment with the ER stress inducing agent Tg. IRE1α was localized to the ER without clustering under homeostatic conditions, while a small number of cells exhibited clusters upon ER stress in control siRNA treated cells (Figure 2A, B, C). By contrast, IRE1α clusters were increased in Sec63 depleted cells treated with ER stress (Figure 2A, B, C). An alternative explanation for IRE1α clustering in Sec63 depleted cells is that it may be caused by defects in protein translocation into the ER in these cells. To rule out this possibility, we performed siRNA

mediated knockdown of Sec62, which is also a core component of the post-translational translocation machinery. Unlike Sec63, transient depletion of Sec62 did not significantly increase IRE1α clusters upon ER stress compared to control siRNA treated cells (Figure 2A, B, C). To further differentiate the role of Sec63 in regulating IRE1α oligomerization from assisting protein translocation into the ER lumen, we used the IRE1α CNX-TMD mutant, which we identified in this study as a Sec61/Sec63 interaction defective mutant (Figure 1B). Consistent with our previous translocon interaction defective IRE1α mutants (Sundaram et al., 2017), the cells expressing IRE1α CNX-TMD displayed significantly more clusters than the cells expressing wild type IRE1α upon treatment with either Tg for 1h and 2h or Tm for 2h (Figure 2D, E). However, both the wild type and IRE1α CNX-TMD formed robust clusters upon treatment of cells with Tm for 4h, although the clusters were slightly bigger in cells expressing the mutant (Figure 2D, E). We next determined if the J-domain of Sec63 is required for limiting IRE1α clustering in cells. The cells expressing Sec63 J-domain mutant (HPD/AAA) exhibited more IRE1α clusters upon ER stress compared to cells expressing wild type Sec63 (Figure 2F, G, H). Taken together, these results suggest that IRE1α forms robust clusters in cells upon ER stress, either if it cannot interact with Sec61/Sec63 or in cells depleted of Sec63.

Sec63 limits IRE1α RNase activity in cells during ER stress

The aforementioned data suggest that Sec63 inhibits the formation of higher-order oligomerization of IRE1α during ER stress. We next wanted to determine if Sec63 also limits IRE1α RNase activity. To test this, we first transiently depleted Sec63 in cells using siRNA oligos and monitored IRE1α activation under homeostatic conditions by probing its phosphorylation status using a phos-tag based immunoblotting. We found that only a small fraction of IRE1α was activated in Sec63 depleted cells under homeostatic conditions (Figure 3 – figure supplement 1A). This small activation was likely caused by defects in protein translocation into the ER in Sec63 depleted cells because a similar level of IRE1α activation was observed in cells depleted of Sec62, which is also a subunit of the protein translocation complex (Figure 3 – figure supplement 1A). To determine the role of Sec63 in suppressing IRE1α activity during ER stress conditions, we monitored IRE1α phosphorylation and its RNase-mediated splicing of XBP1 mRNA in both wild type and Sec63-/- cells treated with Tg. A significant proportion of IRE1α was activated after one hour of ER stress as represented by phosphorylated IRE1α (Figure 3A). Consistent with our previous studies, IRE1α was mostly inactivated or dephosphorylated within eight hours of ER stress in wild type cells. The phosphorylation status of IRE1α was comparable with IRE1α-mediated splicing of XBP1 mRNA (Figure 3A). The ER stress-dependent BiP upregulation was also correlated with the inactivation of IRE1α in wild type cells. Corroborating the result from siRNA-mediated depletion of Sec63, a proportion of IRE1α was constitutively phosphorylated in Sec63-/- cells even under homeostatic conditions. Upon ER stress, IRE1α was fully activated in Sec63-/- cells, but it showed a severe defect in inactivation of IRE1α as reflected by efficient phosphorylation of IRE1α even during the later hours of ER stress compared to wild type cells (Figure 3A). The continuous IRE1α phosphorylation during persistent ER stress correlated with its ability to mediate the splicing of XBP1 mRNA (Figure 3A). Interestingly, although BiP was highly upregulated in Sec63-/- cells (Figure 3 – figure supplement 2C), it could not inactivate IRE1α in the absence of Sec63. We also obtained a similar result when cells were treated with the ER stress inducer Tm (Figure 3 –

figure supplement 1B), arguing against that defective attenuation of IRE1α in Sec63-/- cells was specific to the ER stress inducer Tg.

To exclude the possibility that the knockout of Sec63 had indirect effects on IRE1α activity, we wanted to rescue IRE1α inactivation defects by complementing wild type Sec63 into Sec63-/- cells. The complementation of Sec63 partially restored activation and inactivation kinetics of IRE1α as shown by both IRE1α phosphorylation and XBP1 mRNA splicing (Figure 3B and Figure 3 - figure supplement 1C). By contrast, a proportion of IRE1α was constitutively activated even under homeostatic conditions in Sec63-/- cells complemented with Sec63 J-domain mutant, which is deficient in activating BiP ATPase (Figure 3B and Figure 3 - figure supplement 1C). Upon ER stress, IRE1α was efficiently activated in these cells but could not be attenuated even up to 24h of ER stress, suggesting that the J-domain of Sec63 is required for suppressing IRE1α activity during ER stress. We also complemented Sec63-/- cells with Sec63 mutants (Δ367-760 and Δ637-760) that have intact J-domains but poorly interacted with the Sec61 translocon (Figure 1 – figure supplement 1). These mutants failed to rescue IRE1α attenuation defects observed in Sec63-/- cells during ER stress (Figure 3 – figure supplement 1D). This result implies that Sec63-mediated recruitment of BiP to the ER membrane is not sufficient to inactivate IRE1α, but rather IRE1α must be close to Sec63/BiP for an efficient attenuation of its activity during persistent ER stress. Since Sec63 is involved in protein translocation into the ER, we wanted exclude the possibility that IRE1α attenuation defects were not caused by an inefficient protein translocation into the ER. We therefore created CRISPR/Cas9-mediated knockout cells of Sec62, which did not interact with IRE1α (Figure 1B, C). In sharp contrast to Sec63-/- cells, the activation of IRE1α was mostly inhibited in Sec62-/- cells upon ER stress compared to wild type cells (Figure 3 – figure supplement 1E). Because Sec63 is still present in Sec62-/- cells, it is likely that it can efficiently recruit BiP, which was highly upregulated in these cells, and suppress the activation of IRE1α during ER stress. This notion is supported by our previous study that overexpression of recombinant BiP into HEK293 cells can suppress the activation of endogenous IRE1α (Sundaram et al., 2018).

To determine whether Sec63 also regulates the activities of two other major UPR sensors, PERK and ATF6, we monitored their activation in wild type and Sec63-/- cells during ER stress. Consistent with previous studies, PERK was activated as shown by phosphorylation in wild type cells upon ER stress and remained active throughout the ER stress treatment (Figure 3 – figure supplement 2A, B). We did not detect any appreciable constitutive activation of PERK in Sec63-/- cells under homeostatic conditions. Moreover, it was normally activated upon ER stress induced by either Tg or TM (Figure 3 – figure supplement 2A, B). This result is consistent with the previous study where the depletion of Sec63 did not affect both PERK and ATF6-mediated UPR pathways (Fedeles et al., 2015). We next probed the activation of ATF6 in both wild type and Sec63-/- cells by monitoring the loss of signal due to the proteolytic release of the N-terminal fragment after its migration to the Golgi apparatus (Figure 3 – figure supplement 2A, B). ATF6 signal was lost after one hour of ER stress, but the signal came back after eight hours of the treatment in the wild type cells. To our surprise, ATF6 was poorly activated in Sec63-/- cells during Tg-induced ER stress, but it was noticeably activated upon Tm treatment (Figure 3 – figure supplement 2A, B). We hypothesized that ATF6 was not fully

activated in Sec63-/- cells due to the accumulation of excess of BiP in Sec63-/- cells, which may not be easily sequestered by misfolded proteins induced by the ER stress inducer Tg or Tm. We therefore treated Sec63-/- cells with a strong ER stress inducer, DTT, and monitored ATF6 activation. Indeed, ATF6 could be activated in Sec63-/- cells as shown by the loss of signal upon DTT treatments, suggesting that ATF6 is functional in Sec63-/- cells (Figure 3 – figure supplement 2C). Lastly, we wanted to determine the role of Sec63 in attenuating IRE1α activity using an approach that does not disrupt the function of Sec63 in cells. We therefore monitored IRE1α activity in cells expressing either wild type IRE1α or IRE1α CNX-TMD, which cannot interact with Sec61/Sec63. In support of our conclusion, IRE1α CNX-TMD could be efficiently activated upon ER stress but displayed a defect in attenuation compared to wild type IRE1α as shown by both phosphorylation and XBP1 mRNA splicing during persistent ER stress (Figure 3C). This result is consistent with our previous results of other IRE1α mutants that poorly interact with the Sec61 translocon (Sundaram et al., 2017). Taken together, our data suggest that IRE1α inactivation was significantly impaired during ER stress, either in the absence of Sec63 or if it failed to interact with Sec63.

The Sec61/Sec63 complex recruits BiP to bind onto IRE1α

We next wanted to determine IRE1α binding to BiP depends on its interaction with the Sec61/Sec63 complex. To test this, we took advantage of our various Sec61/Sec63 interaction defective IRE1α mutants (Figure 1B) and performed co-immunoprecipitation studies to monitor their interaction with BiP. Wild type IRE1α associated with BiP along with the Sec61/Sec63 complex, whereas the translocon interaction defective IRE1α mutants showed a significantly less interaction with BiP (Figure 4A). IRE1α mutant that is deleted of the luminal domain (LD) showed a very little binding to BiP, although its interaction with Sec61/Sec63 was mostly unaffected (Figure 4A). This result suggests that BiP binds to the luminal domain of IRE1α, but not to the Sec61/Sec63 complex. To further support our conclusion that IRE1α binds to BiP but not to the Sec61/Sec63 complex, we co-immunoprecipitated IRE1α using either digitonin or NP40/Deoxycholate detergent buffer. IRE1α associated with BiP under both conditions, while its interaction with Sec61/Sec63 was almost abolished when immunoprecipitations were performed using the buffer containing NP40/Deoxycholate compared to the digitonin buffer (Figure 4 – figure supplement 1A, B). The recruitment of BiP to IRE1α was also dependent on the J-domain of Sec63 since overexpression of Sec63 J-domain mutant in cells reduced BiP binding to IRE1α compared to cells overexpressing wild type Sec63 (Figure 4 – figure supplement 1C). We next confirmed whether BiP binding to IRE1α is sensitive to ER stress as previously reported (Bertolotti et al., 2000). Immunoprecipitation of IRE1α from cells treated without or with ER stress induced by DTT, Tg, or Tm revealed that BiP was dissociated from IRE1α under all ER stress conditions compared non-treated cells (Figure 4B). As expected, BiP binding to a translocon interaction defective mutant IRE1α CNX-TMD was significantly reduced even under unstressed conditions, and that the interaction was almost abolished upon treatment with ER stress inducers (Figure 4B). We observed that BiP was upregulated in Tm treated cells compared to DTT or Tg treated cells. This is likely due to the longer time treatment (4h) of Tm while others were treated for a shorter time (2h). We also noticed that IRE1α interaction with Sec63/Sec61 was slightly reduced under ER stress conditions compared to unstressed conditions (Figure 4B). We next asked whether Sec61/Sec63 is necessary and sufficient to

mediate BiP binding to IRE1α. To address this, we purified the IRE1α/Sec61/Sec63 complex from HEK293 cells stably expressing 2xStrep-tagged IRE1α-FLAG as previously described (Sundaram et al., 2017) (Figure 4C). A coomassie stained gel revealed that IRE1α was about three times more than Sec61/Sec63 because the complex was purified from cells overexpressing IRE1α. We also similarly purified IRE1αΔ10, which lacks the interaction with the Sec61/Sec63 complex, as a control. We expressed and purified recombinant BiP from E. coli (Figure 4D). We first prepared anti-FLAG antibody beads bound to the IRE1α complex or IRE1αΔ10. We then incubated the beads with or without BiP in the presence or absence of ATP. In the absence of ATP, BiP bound to both the IRE1α/Sec61/Sec63 complex and IRE1αΔ10. BiP was mostly dissociated from IRE1αΔ10 in the presence of ATP (Figure 4E), likely due to ATP bound BiP has higher substrate dissociation rates (Misselwitz et al., 1998). In sharp contrast, BiP binding to IRE1α/Sec61/Sec63 was intact even in the presence of ATP (Figure 4E). This result suggests that the J-domain of Sec63 stimulated ATP hydrolysis of BiP to bind onto IRE1α. We also obtained a similar result of Sec61/Sec63 dependent BiP binding onto IRE1α when the components were incubated in solution, followed by immunoprecipitation with anti-FLAG beads (Figure 4 – figure supplement 1D). Taken together our results suggest that Sec61/Sec63 is necessary and sufficient to mediate BiP binding to IRE1α in the presence of ATP.

Discussion

We and others have previously shown that IRE1α forms a complex with the Sec61 translocon complex (Plumb et al., 2015; Acosta-Alvear et al., 2018; Ishikawa et al., 2019). The complex formation allows IRE1α to access its substrate mRNAs, including XBP1u mRNA, which is delivered to the Sec61 translocon through its ribosome-nascent chain (Plumb et al., 2015; Kanda et al., 2016). Also, IRE1α association with the Sec61 translocon inhibits its higher-order oligomerization and RNase activity during ER stress (Sundaram et al., 2017). In this study, we show that the translocon associated factor Sec63 recruits and activates BiP ATPase via its luminal J-domain to bind onto IRE1α, thus suppressing higher-order oligomerization and RNase activity of IRE1α during ER stress (Figure 5).

It has long been known that BiP plays a central role in regulating all three UPR sensors (Preissler and Ron, 2019). Recent studies have provided further insights into how BiP regulates oligomerization and activation of IRE1α (Carrara et al., 2015; Kopp et al., 2018; Amin-Wetzel et al., 2017). More recently, the formation of higher-order oligomers or clusters of IRE1α has been shown to be regulated by BiP during ER stress (Ricci et al., 2019). However, it is unclear how the luminal BiP is recruited to the membrane localized IRE1α, which is extremely low abundant (Kulak et al., 2014), to regulate IRE1α oligomerization and activation. Our previous studies have shown that most of the endogenous IRE1α proteins are in complex with the Sec61 translocon complex (Plumb et al., 2015). In this study, we show that Sec63 is a part of the IRE1α/Sec61 translocon complex. Since Sec63 contains a J domain that is known to recruit and activate BiP to bind onto translocating nascent chains (Matlack et al., 1999), we hypothesized that Sec63 recruited BiP might also bind and suppress IRE1α oligomerization and activation. Our interaction studies suggest that the Sec61 translocon bridges the interaction between IRE1α

and Sec63. Although Sec62 is known to associate with Sec63, it is not enriched in IRE1α immunoprecipitates, suggesting that IRE1α selectively interacts with a Sec61 translocon complex that contains Sec63, but not sec62. This is consistent with the depletion of Sec63, but not Sec62, induces the formation of IRE1α clusters upon ER stress. Specifically, the J domain of Sec63 is required for suppressing IRE1α clusters. It is unlikely that IRE1α clustering in Sec63 depleted cells is induced by defects in the protein translocation into the ER since Sec62 depleted cells display less IRE1α clusters upon ER stress. This notion is further supported by our observation that the Sec61/Sec63 interaction defective mutants are able to form robust clusters upon ER stress (Sundaram et al., 2017).

Our studies show that increased levels of IRE1α clusters in Sec63 deficient cells lead to a severe defect in attenuation of IRE1α RNase activity during persistent ER stress. This observation resembles the attenuation defects of IRE1α mutants that cannot efficiently interact with Sec61/Sec63. We envision that such defects in attenuation of IRE1α signaling may be detrimental to cells burdened with high levels of secretory proteins such as pancreatic beta cells (Back and Kaufman, 2012). Surprisingly, Sec63 mutants that have a functional luminal J-domain, but do not interact with the Sec61 translocon also fail to rescue IRE1α attenuation defects in Sec63-/- cells. This result emphasizes that the J-domain containing protein must be close proximal to IRE1α in order to recruit BiP and suppress higher-order oligomerization and RNase activity of IRE1α during ER stress. This view is further supported by our observation that highly upregulated BiP in Sec63-/- cells cannot inhibit the activation of IRE1α during ER stress. Conversely, the activation of IRE1α is completely inhibited in Sec62-/- cells during ER stress, likely due to the presence of Sec63 in these cells can efficiently recruit highly upregulated BiP to bind onto IRE1α.

The ER contains seven J-domain containing proteins localized in the ER lumen where they can interact with BiP (Pobre et al., 2019). It is conceivable that other J-domain containing proteins can compensate the J-domain function of Sec63 in Sec63-/- cells or cells expressing IRE1α mutants that cannot interact with Sec63. Indeed, a small fraction of IRE1α can be attenuated in Sec63-/- cells, but the majority of IRE1α cannot be inactivated during persistent ER stress. Although our data show that Sec63 plays a major role in attenuating IRE1α activity during ER stress, our studies do not provide evidence on whether Sec63 controls the initial activation of IRE1α upon ER stress as the depletion Sec63 only partially activates IRE1α under homeostatic conditions. This partial activation of IRE1α is likely caused by the accumulation of misfolded proteins in the ER lumen since the inhibition of protein synthesis can attenuate IRE1α activity in Sec63 depleted cells (Fedeles et al., 2015).

Two of our experimental evidence suggest that Sec63 is responsible for recruiting luminal BiP to bind and suppress IRE1α higher-order oligomerization and RNase activity during ER stress. First, IRE1α mutants that are deficient in interacting with Sec61/Sec63 show a significantly less binding to BiP. This result also suggests that BiP that binds to IRE1α is mainly recruited through Sec63 in cells. It is possible that these IRE1α mutants also disrupt their interaction with other luminal proteins such as other ERdj proteins. However, this is unlikely since the Sec61/Sec63 interacting region is localized in both luminal juxtamembrane and

transmembrane regions of IRE1α, which should not interfere with IRE1α luminal domain interaction with soluble luminal proteins. Second biochemical reconstitution experiments with purified proteins suggest that Sec61/Sec63 is sufficient and necessary to mediate BiP binding to IRE1α in the presence of ATP. Although BiP binding to IRE1α/Sec61/Sec63 is persistent in the presence of ATP, but its binding to IRE1α is not significantly increased compared to the condition without ATP. This is likely due to three times less amount of Sec63 over IRE1α in our in vitro reactions, while the concentration of Sec63 is vastly abundant than IRE1α in cells (Kulak et al., 2014). Also, the presence of detergent, which is added to keep the membrane proteins soluble, in reactions may disrupt the efficient binding of BiP to IRE1α.

Since the Sec61 translocon selectively associates with the IRE1α branch of the UPR, depletion of Sec63 has less effects on activation PERK and ATF6. This is consistent with previous studies that either depletion of Sec63 or Sec61 selectively activated IRE1α (Adamson et al., 2016; Fedeles et al., 2015). However, ATF6 activation is significantly inhibited in Sec63-/- cells upon ER stress. Although it is not clear the exact cause for this effect, one explanation is that highly upregulated BiP in these cells can effectively suppress ATF6 activation. This notion is supported by our previous studies that the overexpression of recombinant BiP in cells mostly inhibits the activation of ATF6 and IRE1α but has a little effect on the activation of PERK during ER stress (Sundaram et al., 2018). Furthermore, ATF6 in Sec63-/- cells can be activated using the strong ER stress inducer DTT. Since the attenuation kinetics of ATF6 during ER stress closely resembles IRE1α in wild type cells, it may associate with an unknown J-domain protein to recruit and bind onto ATF6, thus preventing its translocation into Golgi when ER stress is alleviated.

Our studies show that IRE1α tightly associates with Sec61/Sec63 through luminal its juxtamembrane and transmebrane regions. Recent structural studies suggest that Sec63 binding to the translocon sterically hinders the ribosome binding to the translocon (Wu et al., 2019; Itskanov and Park, 2019). Future studies are warranted to determine whether Sec63 is dissociated from the translocon when the ribosome-nascent chain complex is recruited to the Sec61/IRE1α complex. Intriguingly, a recent study also shows that IRE1α can directly bind to ribosomes (Acosta-Alvear et al., 2018), suggesting that IRE1α forms an intricate complex with the Sec61 translocon-ribosome complex. Future structural and biochemical studies are needed to visualize this complex to understand how IRE1α monitors and controls protein translocation into the ER.

Materials and methods

Antibodies and Reagents.

Many antibodies and reagents have been previously described (Plumb et al., 2015 and Sundaram et al., 2017). Rabbit anti-Sec61α, anti-Sec62, anti-Sec63, and anti-HA antibodies, Sec62 siRNA, Sec63 siRNA were a generous gift from Dr. Ramanujan Hegde (Medical Research Council, UK). Antibodies purchased: anti-IRE1α (3294, Cell Signaling, Danvers, MA, RRID:AB_ 823545), anti-PERK (3192, Cell Signaling, RRID:AB_2095847), anti-Tubulin

(ab7291, Abcam, Cambridge, UK, RRID:AB_2241126), antiXBP1s (658802, BioLegend, RRID:AB_2562960), anti-BiP (3177, Cell Signaling, Danvers, MA), anti-PERK (Cell Signaling #3192, RRID:AB_2095847), anti-ATF6α (Cell Signaling #65880), Anti-mouse Goat HRP (11-035-003, Jackson Immunoreserach), anti-rabbit Goat HRP (111- 035-003, Jackson Immunoreserach, RRID:AB_2313567), anti-Rabbit Cy3 (711-165-152, Jackson Immuno Research). Resins were purchased: anti-HA magnetic beads (88836, Fisher Scientific, Waltham, MA), anti-FLAG (651503, Biolegend),

Reagents purchased: DMEM (10–013-CV, Corning, Corning, NY), FBS (16000044, Gibco, Gaithersburg, MD), Horse Serum (H0146, Sigma, St Louis, MO), Penicillin/Streptomycin (15140122, Gibco,), Lipofectamine 2000 (11668019, Invitrogen, Carlsbad, CA), Doxycycline (631311, Clontech, Mountain View, CA), Hygromycin (10687010, Invitrogen), Blasticidin (InvivoGen), Thapsigargin (BML-PE180-0005, Enzo Life Sciences, Farmingdale, New York), Protease inhibitor cocktail (11873580001, Roche), poly-L-lysine (OKK-3056, Peptides International), Digitonin (300410, EMD Millipore, Billerica, Massachusetts), Sec62 siRNA (68875, Qiagen), Sec63 siRNA (68711 and 68715, Qiagen), Fluoromount G (0100–01, SouthernBiotech, Birmingham, AL), Phos-tag (300–93523, Wako, Japan), SuperSignal West Pico or Femto Substrate (34080 or 34095, Thermo Scientific). All other common reagents were purchased as indicated in the method section.

DNA constructs,

For mammalian cell expression, cDNAs were cloned into pcDNA5/FRT/TO (Invitrogen, Carlsbad, CA) (Plumb et al., 2015). Constructs encoding IRE1α-HA and its mutants were previously described. The TMD of IRE1α was replaced with calnexin TMD to create IRE1α-CNX-TMD-HA using the protocol previously described (Volmer et al., 2013). Mouse Sec63 plasmid was a kind gift from Dr. Stefan Somlo (Yale School of Medicine). Sec63 truncation constructs, Δ367-760, Δ637-760, Δ230-300, and Δ230-760, were made using phosphorylated primers with the Phusion Site-Directed Mutagenesis protocol. The tripeptide HPD in the J-domain was replaced with AAA to create the J-domain mutant of Sec63 using site-directed mutagenesis (Zheng et al., 2004). Rat BiP lacking the N-terminal signal sequence (1-18 amino acids) was cloned into pET-28a (+) using a standard cloning procedure. 3% DMSO was included in all PCR reactions to enhance amplification. The coding regions of all constructs were verified by sequencing performed in the Yale Keck DNA Sequencing Facility.

Cell culture and stable cell lines

HEK 293-Flp-In T-Rex cells (Invitrogen) were cultured in high glucose DMEM containing 10% FBS at 5% CO2. HEK293 IRE1α-/- cells stably expressing IRE1α-HA, IRE1α-CNX-TMD-HA were generated as previously described (Plumb et al., 2015). HEK293 cells stably expressing 2xStrep-IRE1α-FLAG or 2xStrep-IRE1α Δ10-FLAG were previously described (Sundaram et al., 2017). To establish HEK293 Sec63-/- cells stably expressing either IRE1α variants or Sec63 variants were created by transfecting with 1.5μg of pOG44 vector (Invitrogen) and 0.5μg of FRT vectors containing IRE1α or Sec63 using Lipofectamine 2000 (Invitrogen). After transfection, cells were plated in 150 μg/ml hygromycin (Invitrogen) and 10 μg/ml blasticidin (InvivoGen, San

Diego, CA). The medium was replaced every three days until colonies appeared. The colonies were picked and the protein expression was evaluated by immunoblotting. We have not tested the cell lines used in this study for the presence of mycoplasma, but many cell lines were used in immunofluorescence assays with Hoechst staining that should reveal presence of mycoplasma. The cells were assumed to be authenticated by their respective suppliers and were not further confirmed in this study. However, Sec63 knock out cell lines were verified by immunoblotting with anti-Sec63 antibodies.

CRISPR/Cas9-mediated knock out cell lines

IRE1α-/- HEK293-Flp-In T-Rex cells created by CRISPR/Cas9 were previously described (Plumb et al., 2015). The human Sec63 targeting sequence (5′ GTGTATGTGGTATCGTTTA 3′) or human Sec62 targeting sequence (5′ AGTATCTTCGATTCAACTG 3′) was cloned into the gRNA expression vector (Mali et al., 2013) in order to direct Cas9 nuclease activity. HEK 293-Flp-In T-Rex cells were plated in a six-well plate and transfected at 70% confluence with 500 ng of the gRNA expression vector and 500 ng of the pSpCas9(BB)-2A-Puro (Ran et al., 2013) plasmid with Lipofectamine 2000. Expression of Cas9 was selected by puromycin treatment (2.5 µg/ml) for 48 hr, after which cells were returned to non-selecting media for 72 hr. Cells were then plated at 0.5 cell/well in 96 well plates and expanded for 3 weeks. Individual clones were examined for Sec63 or Sec62 by immunoblotting.

Immunoprecipitations

To test the interaction between IRE1α and the Sec61 translocon complex, 0.8 million HEK 293 cells were plated on a poly-L-lysine (0.1mg/ml) coated 6 well plate. The cells were transiently transfected with 2µg of HA-tagged or FLAG-tagged constructs using 5µl of lipofectamine 2000 and treated with 100 ng/ml doxycycline unless otherwise indicated in the figure legends to induce protein expression. 24 hr after transfection, cells were harvested in 1xPBS and centrifuged for 2 min at 10,000g. The cell pellet was lysed in 200ul of Buffer A (50 mM Tris pH 8.0, 150 mM NaCl, 5 mM MgAc) including 2% digitonin by incubating on ice for 30min. The 5% digitonin (EMD Millipore) stock was boiled for 5 min just before adding into Buffer A to avoid digitonin precipitating during IP. The supernatant was collected by centrifugation at 15,000*g* for 15 min. For co-immunoprecipitation, the supernatant was rotated with 12µl anti-FLAG-agarose (Biolegend) or 15µl anti-HA magnetic beads (Thermo Scientific) for 1h 30min in the cold room. The beads were washed 3x with 1 ml of Buffer A including 0.1% digitonin. The bound material was eluted from the beads by directly boiling in 50 µl of 2x SDS sample buffer for 5 min and analyzed by immunoblotting.

To test the interaction between BiP and IRE1α, 0.8 million cells were plated on a 6 well plate and transiently transfected with 2µg of IRE1α or its variants. The cells were washed and harvested in 1xPBS and centrifuged for 2 min at 10,000*g*. The cell pellet was lysed in either 200ul of Buffer A including 2% digitonin or NP40 buffer (50 mM Tris, pH 7.5, 150 mM NaCl, 0.5% deoxycholic acid, and 0.5% NP40). Apyrase (10 U/ml) and 10 mM CaCl2 were included in both buffers and incubated for 30 min on ice. The cell lysate was centrifuged at 15,000*g* for 15 min. The supernatant was incubated with anti-HA magnetic beads (Thermo Scientific) for 1h 30 min in the cold room. The beads were washed 3 times with either 1ml of Buffer A including 0.1% digitonin or 1 ml of NP40 buffer and eluted by directly boiling in 50 µl of 2x SDS sample buffer

for 5 min and analyzed by immunoblotting. In Figure 4B, HEK293 IRE1α-/- cells complemented with IRE1α-HA or IRE1α CNX-TMD-HA were plated as above and induced with 1ng of Doxycycline for overnight. The cells were harvested, immunoprecipitated, and analyzed as above.

Purification of the IRE1α/Sec61/Sec63 complex, IRE1α Δ10, and BiP

The IRE1α/Sec61/Sec63 complex and IRE1αΔ10 were purified as described previously (Sundaram et al., 2017). Briefly, microsomes were prepared from HEK293 cells stably expressing either 2xStrep IRE1α-FLAG or 2xStrep IRE1α Δ10-FLAG as described previously. 2ml of microsomes (OD280 = 50) were lysed with an equal volume of lysis buffer (50 mM Tris pH8, 600 mM NaCl, 5 mM MgCl2, 2% digitonin (boiled prior to use) 1x protease inhibitor cocktail and 10% glycerol) by incubating 30min on ice. The lysates were centrifuged at 25 000g for 25 min at 4°C. Supernatant was collected and passed through a column packed with 1ml of compact StrepTactin beads (IBA, Germany) by gravity flow. Flow-through was collected and beads were washed with 6x 1ml of wash buffer (50 mM Tris pH 8.0, 150 mM NaCl, 5 mM MgCl2, 10% Glycerol and 0.1% digitonin). 2xStrep IRE1α or IRE1α Δ10-FLAG was eluted from the beads using 20 mM desthiobiotin (EMD Millipore) included in the wash buffer. The desthiobiotin eluted material was further purified by passing through a cation exchange chromatography (SP Sepharose beads, GE Healthcare). Briefly beads were prepared in a 2 ml Bio-Rad column and washed 5x using no salt buffer (20 mM Tris pH 6.0, 2 mM MgAc and 0.4% DBC). Purified protein was diluted 5x with no salt buffer and pass-through the S-column. Beads were washed 5x column volume with no salt buffer and eluted with 500 mM NaCl buffer (50 mM Tris pH8, 2 mM MgAc, 10% glycerol, and 0.4% DBC). BiP that is bound to IRE1α is mostly removed by this step because BiP does not bind to a cation exchange resin. Purified IRE1α/Sec63/Sec61 or IRE1α Δ10 were subjected to coomassie staining and quantified using BSA standards (Sigma).

The pET-28a (+) plasmid encoding N-terminally 6X His-tagged rat BiP lacking the N-terminal signal sequence was expressed and purified from E. coli as descripted by Amin-Wetzel et al., 2017. Briefly, pET-28a (+) His-BiP was transformed into BL21 Rosetta (DE3) cells. The overnight culture of His-BiP was inoculated into fresh liquid LB and grown to OD600 of ~ 0.8 at 37°C. The culture was cooled down to 18°C and induce with 0.5mM imidazole. After 16h induction, the cells were harvested and resuspended with buffer A (50 mM Tris pH7.4, 500 mM NaCl, 10% glycerol, 1 mM MgCl2, 0.2% (v/v) Triton X-100, 20 mM imidazole). The suspension was passed through the high-pressure homogenizer for 4 times. The lysate was spun at 35000rpm for 40min at 4°C using Ti45 rotor. The supernatant was incubated with the prewashed 2mL of Ni-NTA beads and washed with 20ml of Buffer B (50 mM Tris pH 7.4, 500 mM NaCl, 10% glycerol, 1 mM MgCl2, 0.2% (v/v) Triton X-100, 30 mM imidazole). Subsequently, the column was washed with 10ml of Buffer C (50 mM Tris pH 7.4, 1M NaCl, 10% glycerol, 5 mM MgCl2, 1% (v/v) Triton X-100, 30 mM imidazole, 5mM ATP) and further washed with 10ml of Buffer D (50 mM Tris pH 7.4, 500 mM NaCl, 10% glycerol, 1 mM MgCl2, 30 mM imidazole).The bound proteins were eluted with Buffer E (50 mM Tris pH 7.4, 500 mM NaCl, 10% glycerol, 1 mM MgCl2, 250 mM imidazole). The peak fractions containing BiP was

pooled and dialyzed against Buffer F (50 mM Tris pH 7.4, 150 mM NaCl, 10% glycerol, 5 mM MgCl2, 1mM CaCl2). The purified proteins were flash frozen and stored at -80°C.

In vitro reconstitution of Sec61/Sec63-mediated BiP binding to IRE1α

IRE1α binding to BiP was adapted from Amin-Wetzel et al., 2017 with the following modifications. 12μl of Anti-FLAG beads was incubated with either 0.15μg of the 2X Strep-IRE1α-FLAG/Sec61/Sec63 complex or 0.15μg of 2X Strep-IRE1α Δ10-FLAG in 500ul of wash buffer (50 mM Tris pH 8.0, 150 mM NaCl, 10 mM MgCl2, 0.4% DBC) for 1h at 4°C. The beads were washed twice with 1ml of wash buffer. IRE1α bound beads were resuspended with 50ul of binding buffer (50 mM Tris pH 8.0, 150 mM NaCl, 10 mM MgCl2, 1mM CaCl2, 0.1% Triton X-100) including either BiP (1μg) and ATP (2mM). A negative control reaction was performed by incubating empty anti-FLAG beads with the buffer, BiP, and ATP. After incubation at 32°C for 30 min, the beads were quickly washed with ice-cold wash buffer including 2mM ADP. The wash was repeated one more time with wash buffer excluding ADP. The bound proteins were eluted from beads 50μl of 2X SDS sample buffer and analyzed by immunoblotting. We used the following protocol to BiP binding to IRE1α in Figure 4 – figure supplement 2. 0.15μg of the 2X Strep-IRE1α-FLAG/Sec61/Sec63 complex or 0.15μg of 2X Strep-IRE1α Δ10-FLAG was incubated with and without 5μg BiP in 50ul of binding buffer (50 mM Tris pH 8.0, 100 mM NaCl, 10 mM MgCl2, 1mM CaCl2, 2mM ATP, 0.2% DBC) for 30min at 32°C. A negative control reaction was performed by mixing the buffer, BiP, and ATP. The reactions were terminated by diluting with ice-cold NP40 buffer (50 mM Tris, pH 7.5, 150 mM NaCl, 0.5% deoxycholic acid, and 0.5% NP40) and incubated with 12μl of anti-FLAG beads for 1h 30min at 4°C. After incubation, the beads were washed twice with 1ml of NP40 buffer. The bound proteins were eluted by boiling beads with 50μl of SDS sample buffer and analyzed by immunoblotting.

Immunofluorescence

HEK293 IRE1α-/- cells stably complemented with IRE1α-HA (0.12 X 10^6) were plated on 12 mm round glass coverslips (Fisher Scientific) coated with 0.1 mg/mL poly-lysine for 5 hr in 24-well plates. For Figure 2A, the cells expressing IRE1α-HA were transfected with either 20 pmole of Sec62 siRNA or Sec63 siRNA using 2μl of lipofectamine 2000 and induced with 5ng/ml of doxycycline to induce IRE1α expression. After 30 hr of transfection, cells were treated with 5 μg/ml of thapsigargin (Tg) for 1.5 h before fixing and immunostaining as described previously (Sundaram et al., 2017). For Figure 2D, HEK293 IRE1α-/- cells stably expressing either WT IRE1α-HA or IRE1α CNX-TMD-HA were induced with 5ng/ml doxycycline and treated with 5 μg/ml of Tm or Tg for the indicated time points. The treated cells were fixed and processed for immunostaining. For Figure 2F, the cells expressing IRE1α-HA were transfected with 0.1μg of Sec63 or Sec63 HPD/AAA using 1μl of lipofectamine 2000. IRE1α expression was induced with doxycycline (5ng/ml) for 16 hr before treatment with 5 μg/ml Tg for 1.5 h followed by fixed and immunostained with anti-HA antibodies for IRE1α. The cells were imaged on Leica scanning confocal microscope and IRE1α clusters were quantified as previously described (Sundaram et al., 2017) with the following modifications. For each condition, we randomly chose at least 10 fields-of-view and took images. First, we identified the total number of cells per frame by manually counting Hoechst-stained nuclei. We counted more than 300 cells from the 10 images

of each condition and looked for cells with IRE1α clusters. Of those cells, we calculated the percentage of cells with IRE1α clusters. Data was graphed using GraphPad Prism and represented with standard error of the mean from two independent experiments.

XBP1 mRNA splicing assay

Total RNA was extracted from cells using Trizol reagent (Ambion) according to the manufactures protocol. 2μg of total RNA was treated with 1U/ul DNase I (Promega). 0.5μg of DNAse-treated RNA was reverse transcribed into cDNA using Oligo(dT)20 primer (Qiagen) and M-MLUV reverse transcriptase (NEB). cDNA was amplified by standard PCR with TaqDNA polymerase using the primers: 5'-AAACAGAGTAGCAGCTCAGACTGC -3', 5'-TCCTTCTGGGTAGACCTCTGGGAG -3' (Calfon et al., 2002). PCR products of XBP1 were resolved by 2% agarose gel and stained with ethidium bromide. The intensities of DNA bands were quantified on image analyzer (Image J, NIH).

Phostag-based immunoblotting

Typically, 0.15 X 10^6 cells were plated on 24 well poly-lysine coated plates. The following day, cells were treated with 5μg/ml Tg for various time points indicated in Figure 3. The cells were directly harvested in 100 ul of 2X sample buffer and boiled for 5 to 10 minutes. IRE1α phosphorylation was detected by the previously described method (Yang et al., 2010). Briefly, 5% SDS PAGE gel was made using 25 μM Phos-tag (Wako). SDS-PAGE was run at 100 V for 2 hr and 30 min. The gel was transferred to nitrocellulose (Bio-Rad, Hercules, CA) and followed with immunoblotting. The intensities of the Phos-tag bands were quantified on image analyzer (Image J, NIH). To probe the phosphorylation of PERK, the samples were run on a 7.5% Tris/Tricine gel for 2 h and 30 min and transferred to nitrocellulose membrane and blotted using a standard procedure.

Acknowledgments

We thank Dr. Ramanujan Hegde for Sec62 and Sec63 antibodies, and Dr. Stefan Somlo for mouse Sec63 plasmid. We thank Jacob Culver for useful discussion and comments on the manuscript. This work is funded by NIH grants R01GM117386 (M.M) and R21AG056800 (M.M).

References

Acosta-Alvear, D., G.E. Karagoz, F. Frohlich, H. Li, T.C. Walther, and P. Walter. 2018. The unfolded protein response and endoplasmic reticulum protein targeting machineries converge on the stress sensor IRE1α. Elife. 7.

Adamson, B., T.M. Norman, M. Jost, M.Y. Cho, J.K. Nunez, Y. Chen, J.E. Villalta, L.A. Gilbert, M.A. Horlbeck, M.Y. Hein, R.A. Pak, A.N. Gray, C.A. Gross, A. Dixit, O. Parnas, A. Regev, and J.S. Weissman. 2016. A Multiplexed Single-Cell CRISPR Screening Platform Enables Systematic Dissection of the Unfolded Protein Response. Cell. 167:1867-1882 e1821.

Alder, N.N., Y. Shen, J.L. Brodsky, L.M. Hendershot, and A.E. Johnson. 2005. The molecular mechanisms underlying BiP-mediated gating of the Sec61 translocon of the endoplasmic reticulum. J Cell Biol. 168:389-399.

Amin-Wetzel, N., R.A. Saunders, M.J. Kamphuis, C. Rato, S. Preissler, H.P. Harding, and D. Ron. 2017. A J-Protein Co-chaperone Recruits BiP to Monomerize IRE1α and Repress the Unfolded Protein Response. Cell. 171:1625-1637 e1613.

Back, S.H., and R.J. Kaufman. 2012. Endoplasmic reticulum stress and type 2 diabetes. Annu Rev Biochem. 81:767-793.

Bertolotti, A., Y. Zhang, L.M. Hendershot, H.P. Harding, and D. Ron. 2000. Dynamic interaction of BiP and ER stress transducers in the unfolded-protein response. Nat Cell Biol. 2:326-332.
Brodsky, J.L. 2012. Cleaning up: ER-associated degradation to the rescue. Cell. 151:1163-1167.

Brodsky, J.L., J. Goeckeler, and R. Schekman. 1995. BiP and Sec63p are required for both co- and posttranslational protein translocation into the yeast endoplasmic reticulum. Proc Natl Acad Sci U S A. 92:9643-9646.

Calfon, M., H. Zeng, F. Urano, J.H. Till, S.R. Hubbard, H.P. Harding, S.G. Clark, and D. Ron. 2002. IRE1α couples endoplasmic reticulum load to secretory capacity by processing the XBP-1 mRNA. Nature. 415:92-96.

Carrara, M., F. Prischi, P.R. Nowak, M.C. Kopp, and M.M. Ali. 2015. Noncanonical binding of BiP ATPase domain to Ire1 and Perk is dissociated by unfolded protein CH1 to initiate ER stress signaling. Elife. 4.

Conti, B.J., P.K. Devaraneni, Z. Yang, L.L. David, and W.R. Skach. 2015. Cotranslational stabilization of Sec62/63 within the ER Sec61 translocon is controlled by distinct substrate-driven translocation events. Mol Cell. 58:269-283.

Cox, J.S., C.E. Shamu, and P. Walter. 1993. Transcriptional induction of genes encoding endoplasmic reticulum resident proteins requires a transmembrane protein kinase. Cell. 73:1197-1206.

Cubillos-Ruiz, J.R., S.E. Bettigole, and L.H. Glimcher. 2017. Tumorigenic and Immunosuppressive Effects of Endoplasmic Reticulum Stress in Cancer. Cell. 168:692-706.

Deshaies, R.J., S.L. Sanders, D.A. Feldheim, and R. Schekman. 1991. Assembly of yeast Sec proteins involved in translocation into the endoplasmic reticulum into a membrane-bound multisubunit complex. Nature. 349:806-808.

Eletto, D., D. Eletto, D. Dersh, T. Gidalevitz, and Y. Argon. 2014. Protein disulfide isomerase A6 controls the decay of IRE1αalpha signaling via disulfide-dependent association. Mol Cell. 53:562-576.

Ghosh, R., L. Wang, E.S. Wang, B.G. Perera, A. Igbaria, S. Morita, K. Prado, M. Thamsen, D. Caswell, H. Macias, K.F. Weiberth, M.J. Gliedt, M.V. Alavi, S.B. Hari, A.K. Mitra, B. Bhhatarai, S.C. Schurer, E.L. Snapp, D.B. Gould, M.S. German, B.J. Backes, D.J. Maly, S.A. Oakes, and F.R. Papa. 2014. Allosteric inhibition of the IRE1αalpha RNase preserves cell viability and function during endoplasmic reticulum stress. Cell. 158:534-548.

Han, D., A.G. Lerner, L. Vande Walle, J.P. Upton, W. Xu, A. Hagen, B.J. Backes, S.A. Oakes, and F.R. Papa. 2009. IRE1αalpha kinase activation modes control alternate endoribonuclease outputs to determine divergent cell fates. Cell. 138:562-575.

Harding, H.P., Y. Zhang, and D. Ron. 1999. Protein translation and folding are coupled by an endoplasmic-reticulum-resident kinase. Nature. 397:271-274.

Haze, K., H. Yoshida, H. Yanagi, T. Yura, and K. Mori. 1999. Mammalian transcription factor ATF6 is synthesized as a transmembrane protein and activated by proteolysis in response to endoplasmic reticulum stress. Mol Biol Cell. 10:3787-3799.

Hetz, C. 2012. The unfolded protein response: controlling cell fate decisions under ER stress and beyond. Nat Rev Mol Cell Biol. 13:89-102.

Hollien, J., and J.S. Weissman. 2006. Decay of endoplasmic reticulum-localized mRNAs during the unfolded protein response. Science. 313:104-107.

Ishikawa, Y., S. Fedeles, A. Marlier, C. Zhang, A.R. Gallagher, A.H. Lee, and S. Somlo. 2019. Spliced XBP1 Rescues Renal Interstitial Inflammation Due to Loss of Sec63 in Collecting Ducts. J Am Soc Nephrol.

Itskanov, S., and E. Park. 2019. Structure of the posttranslational Sec protein-translocation channel complex from yeast. Science. 363:84-87.

Jurkin, J., T. Henkel, A.F. Nielsen, M. Minnich, J. Popow, T. Kaufmann, K. Heindl, T. Hoffmann, M. Busslinger, and J. Martinez. 2014. The mammalian tRNA ligase complex mediates splicing of XBP1 mRNA and controls antibody secretion in plasma cells. EMBO J. 33:2922-2936.

Kopp, M.C., P.R. Nowak, N. Larburu, C.J. Adams, and M.M. Ali. 2018. In vitro FRET analysis of IRE1α and BiP association and dissociation upon endoplasmic reticulum stress. Elife. 7.

Kosmaczewski, S.G., T.J. Edwards, S.M. Han, M.J. Eckwahl, B.I. Meyer, S. Peach, J.R. Hesselberth, S.L. Wolin, and M. Hammarlund. 2014. The RtcB RNA ligase is an essential component of the metazoan unfolded protein response. EMBO Rep. 15:1278-1285.

Kulak, N.A., G. Pichler, I. Paron, N. Nagaraj, and M. Mann. 2014. Minimal, encapsulated proteomic-sample processing applied to copy-number estimation in eukaryotic cells. Nat Methods. 11:319-324.

Lee, A.H., N.N. Iwakoshi, and L.H. Glimcher. 2003. XBP-1 regulates a subset of endoplasmic reticulum resident chaperone genes in the unfolded protein response. Mol Cell Biol. 23:7448-7459.

Li, H., A.V. Korennykh, S.L. Behrman, and P. Walter. 2010. Mammalian endoplasmic reticulum stress sensor IRE1α signals by dynamic clustering. Proc Natl Acad Sci U S A. 107:16113-16118.

Lin, J.H., H. Li, D. Yasumura, H.R. Cohen, C. Zhang, B. Panning, K.M. Shokat, M.M. Lavail, and P. Walter. 2007. IRE1α signaling affects cell fate during the unfolded protein response. Science. 318:944-949.

Lu, Y., F.X. Liang, and X. Wang. 2014. A synthetic biology approach identifies the mammalian UPR RNA ligase RtcB. Mol Cell. 55:758-770.

Mali, P., L. Yang, K.M. Esvelt, J. Aach, M. Guell, J.E. DiCarlo, J.E. Norville, and G.M. Church. 2013. RNA-guided human genome engineering via Cas9. Science. 339:823-826.

Meyer, H.A., H. Grau, R. Kraft, S. Kostka, S. Prehn, K.U. Kalies, and E. Hartmann. 2000. Mammalian Sec61 is associated with Sec62 and Sec63. J Biol Chem. 275:14550-14557.

Misselwitz, B., O. Staeck, and T.A. Rapoport. 1998. J proteins catalytically activate Hsp70 molecules to trap a wide range of peptide sequences. Mol Cell. 2:593-603.

Mori, K., W. Ma, M.J. Gething, and J. Sambrook. 1993. A transmembrane protein with a cdc2+/CDC28-related kinase activity is required for signaling from the ER to the nucleus. Cell. 74:743-756.

Okamura, K., Y. Kimata, H. Higashio, A. Tsuru, and K. Kohno. 2000. Dissociation of Kar2p/BiP from an ER sensory molecule, Ire1p, triggers the unfolded protein response in yeast. Biochem Biophys Res Commun. 279:445-450.

Panzner, S., L. Dreier, E. Hartmann, S. Kostka, and T.A. Rapoport. 1995. Posttranslational protein transport in yeast reconstituted with a purified complex of Sec proteins and Kar2p. Cell. 81:561-570.

Pincus, D., M.W. Chevalier, T. Aragon, E. van Anken, S.E. Vidal, H. El-Samad, and P. Walter. 2010. BiP binding to the ER-stress sensor Ire1 tunes the homeostatic behavior of the unfolded protein response. PLoS Biol. 8:e1000415.

788 Plumb, R., Z.R. Zhang, S. Appathurai, and M. Mariappan. 2015. A functional link between the
789 co-translational protein translocation pathway and the UPR. Elife. 4.
790
791 Pobre, K.F.R., G.J. Poet, and L.M. Hendershot. 2019. The endoplasmic reticulum (ER)
792 chaperone BiP is a master regulator of ER functions: Getting by with a little help from ERdj
793 friends. J Biol Chem. 294:2098-2108.
794
795 Poothong, J., W. Tirasophon, and R.J. Kaufman. 2017. Functional analysis of the mammalian
796 RNA ligase for IRE1α in the unfolded protein response. Biosci Rep. 37.
797
798 Preissler, S., and D. Ron. 2019. Early Events in the Endoplasmic Reticulum Unfolded Protein
799 Response. Cold Spring Harb Perspect Biol. 11.
800
801 Ran, F.A., P.D. Hsu, J. Wright, V. Agarwala, D.A. Scott, and F. Zhang. 2013. Genome
802 engineering using the CRISPR-Cas9 system. Nat Protoc. 8:2281-2308.
803
804 Rapoport, T.A. 2007. Protein translocation across the eukaryotic endoplasmic reticulum and
805 bacterial plasma membranes. Nature. 450:663-669.
806
807 Ricci, D., I. Marrocco, D. Blumenthal, M. Dibos, D. Eletto, J. Vargas, S. Boyle, Y.
808 Iwamoto, S. Chomistek, J.C. Paton, A.W. Paton, and Y. Argon. 2019. Clustering of
809 IRE1α alpha depends on sensing ER stress but not on its RNase activity. Faseb
810 Journal. 33:9811-9827.
811
812 Sepulveda, D., D. Rojas-Rivera, D.A. Rodriguez, J. Groenendyk, A. Kohler, C. Lebeaupin, S.
813 Ito, H. Urra, A. Carreras-Sureda, Y. Hazari, M. Vasseur-Cognet, M.M.U. Ali, E. Chevet, G.
814 Campos, P. Godoy, T. Vaisar, B. Bailly-Maitre, K. Nagata, M. Michalak, J. Sierralta, and C.
815 Hetz. 2018. Interactome Screening Identifies the ER Luminal Chaperone Hsp47 as a Regulator
816 of the Unfolded Protein Response Transducer IRE1αalpha. Mol Cell. 69:238-252 e237.
817
818 Shao, S., and R.S. Hegde. 2011. Membrane protein insertion at the endoplasmic reticulum.
819 Annu Rev Cell Dev Biol. 27:25-56.
820
821 Shoulders, M.D., L.M. Ryno, J.C. Genereux, J.J. Moresco, P.G. Tu, C. Wu, J.R. Yates, 3rd, A.I.
822 Su, J.W. Kelly, and R.L. Wiseman. 2013. Stress-independent activation of XBP1s and/or ATF6
823 reveals three functionally diverse ER proteostasis environments. Cell Rep. 3:1279-1292.
824
825 Sood, R., A.C. Porter, K. Ma, L.A. Quilliam, and R.C. Wek. 2000. Pancreatic eukaryotic initiation
826 factor-2alpha kinase (PEK) homologues in humans, Drosophila melanogaster and
827 Caenorhabditis elegans that mediate translational control in response to endoplasmic reticulum
828 stress. Biochem J. 346 Pt 2:281-293.
829

Sundaram, A., S. Appathurai, R. Plumb, and M. Mariappan. 2018. Dynamic changes in complexes of IRE1αalpha, PERK, and ATF6alpha during endoplasmic reticulum stress. Mol Biol Cell. 29:1376-1388.

Sundaram, A., R. Plumb, S. Appathurai, and M. Mariappan. 2017. The Sec61 translocon limits IRE1αalpha signaling during the unfolded protein response. Elife. 6.

van Anken, E., and I. Braakman. 2005. Versatility of the endoplasmic reticulum protein folding factory. Crit Rev Biochem Mol Biol. 40:191-228.

Volmer, R., K. van der Ploeg, and D. Ron. 2013. Membrane lipid saturation activates endoplasmic reticulum unfolded protein response transducers through their transmembrane domains. Proc Natl Acad Sci U S A. 110:4628-4633.

Walter, P., and D. Ron. 2011. The unfolded protein response: from stress pathway to homeostatic regulation. Science. 334:1081-1086.

Wang, M., and R.J. Kaufman. 2016. Protein misfolding in the endoplasmic reticulum as a conduit to human disease. Nature. 529:326-335.

Wu, X., C. Cabanos, and T.A. Rapoport. 2019. Structure of the post-translational protein translocation machinery of the ER membrane. Nature. 566:136-139.

Yang, L., Z. Xue, Y. He, S. Sun, H. Chen, and L. Qi. 2010. A Phos-tag-based approach reveals the extent of physiological endoplasmic reticulum stress. PLoS One. 5:e11621.

Ye, J., R.B. Rawson, R. Komuro, X. Chen, U.P. Dave, R. Prywes, M.S. Brown, and J.L. Goldstein. 2000. ER stress induces cleavage of membrane-bound ATF6 by the same proteases that process SREBPs. Mol Cell. 6:1355-1364.

Yoshida, H., T. Matsui, A. Yamamoto, T. Okada, and K. Mori. 2001. XBP1 mRNA is induced by ATF6 and spliced by IRE1α in response to ER stress to produce a highly active transcription factor. Cell. 107:881-891.

Young, B.P., R.A. Craven, P.J. Reid, M. Willer, and C.J. Stirling. 2001. Sec63p and Kar2p are required for the translocation of SRP-dependent precursors into the yeast endoplasmic reticulum in vivo. EMBO J. 20:262-271.

Zheng, L., U. Baumann, and J.L. Reymond. 2004. An efficient one-step site-directed and site-saturation mutagenesis protocol. Nucleic Acids Res. 32:e115.

Figure Legends

Figure 1. The Sec61 translocon bridges the interaction between IRE1α and Sec63
(**1**) A diagram showing the Sec61 translocon interaction region in IRE1α. Triangle depicts amino acid residues of IRE1α that are important for the interaction with the Sec61 translocon (Plumb et al., 2015). (**B**) The cell lysates of the indicated versions of HA-tagged IRE1α were immunoprecipitated using an anti-HA antibody, eluted with sample buffer, and analyzed by immunoblotting. IRE1α Δ10 lacks amino acids 434 to 443 in human IRE1α. IRE1α VD/AA, L/A, and M/A are mutations within the 10-amino acid region shown in panel A. The TMD of IRE1α is replaced with the TMD of calnexin in the IRE1α CNX-TMD construct. (**C**) HEK293 or HEK293 Sec63-/- cells were transfected with either wild type IRE1α-HA or IRE1α Δ10-HA and immunoprecipitated using an anti-HA antibody and eluted with sample buffer. The immunoprecipitates were analyzed by immunoblotting for the indicated antigens. The amount of IRE1α bound to Sec61α was takedn as 100%. (**D**) The cell lysates from FLAG-tagged wild type (WT) Sec63, the J-domain mutant, and Δ230-300 were immunoprecipitated using an anti-FLAG antibody and immunoblotted for the indicated antigens. (**E**) Sec63-/- cells complemented with Sec63-FLAG were either treated with DMSO, 5ug/ml thapsigargin (Tg) or 5ug/ml tunicamycin (Tm) for 4h. The DTT treatment was done with 4mM for either 4h or 8h. Sec63 was immunoprecipitated from these cell lysates and immunoblotted for the indicated antigens. The amount of IRE1α bound to Sec63 from DMSO treated sample was set as 100%. The percentage of IRE1α bound to Sec63 upon Tg, Tm, or DTT treated sample was calculated with respect to the DMSO treated sample.

Figure 1 – figure supplement 1. IRE1α interacts with Sec63 through the Sec61 translocon
(**A**) A diagram showing the topology of Sec63. (**B**) The cell lysates of the indicated versions of FLAG-tagged Sec63 were immunoprecipitated with anti-FLAG beads and analyzed by immunoblotting for the indicated antigens. The HPD tripeptide in the J-domain was replaced with AAA to create the J-domain mutant of Sec63.

Figure 2. Sec63 inhibits IRE1α clustering during ER stress in cells.
(**A**) HEK293 IRE1α-/- cells complemented with IRE1α-HA were transfected with either control, Sec63, or Sec62 siRNA. The expression of IRE1α-HA was induced with 5ng/ml doxycycline. After 30h of transfection, the cells were either left untreated or treated with 5μg/ml Tg for 1.5h and processed for immunostaining with anti-HA antibodies for IRE1α. Scale bars are 10 μm. (**B**) Quantification of the number of cells with IRE1α clusters from the panel A. Error bar represents standard deviation (n=2). (**C**) HEK293 IRE1α-/- cells were treated with the indicated siRNAs. After 30h of transfection, the cells were harvested and analyzed by immunoblotting for the indicated antigens. (**D**) HEK293 IRE1α-/- cells expressing either IRE1α-HA or IRE1α-CNX-TMD-HA were induced with 5ng/ml doxycycline and treated with either Tg or Tm for the indicated time points. The cells were then processed for immunostaining as in A. (**E**) The number of cells with IRE1α clusters were quantified from the panel D. Error bar represents standard deviation (n=2). (**F**) HEK293 IRE1α-/- cells expressing IRE1α-HA were transfected with either empty vector, wild type (WT) Sec63 or the J-domain mutant of Sec63. The expression of IRE1α-HA was induced with 5ng/ml doxycycline. After 24h of transfection, the cells were either left untreated or treated with 5μg/ml Tg for 1.5h and subsequently processed for immunostaining with anti-HA antibodies

for IRE1α. (**G**) Quantification of the number of cells with IRE1α clusters from the panel F. Error bar represents standard deviation (n=2) (**H**) The cells were transfected as in the panel F, but analyzed by immunoblotting for the indicated antigens.

Figure 3. The J domain of Sec63 is essential for attenuating IRE1α activity during ER stress in cells.

(**A**) Wild type HEK293 or Sec63-/- cells were treated with 5μg/ml of Tg for the indicated time points and analyzed by immunoblotting as well as the XBP1 mRNA splicing assay. p-IRE1α denotes the phosphorylated form of IRE1α, which migrates slower in the phos-tag immunoblotting. The percentage of IRE1α phosphorylation is shown underneath phos-tag immunoblots. The percentage of spliced XBP1 mRNA is shown underneath agarose gels. XBP1u - Unspliced XBP1 mRNA, XBP1s - spliced XBP1 mRNA. (**B**) Sec63-/- cells complemented with either WT or the J-domain mutant of IRE1α were treated and analyzed as in the panel A. (**C**) HEK293 IRE1α-/- cells stably complemented with either WT IRE1α or IRE1α-CNX-TMD were treated with 5μg/ml of Tg for the indicated time points and analyzed by immunoblots as well as the XBP1 mRNA splicing assay.

Figure 3 – figure supplement 1: Sec63 but not Sec62 is required for attenuating IRE1α RNase activity during ER stress.

(**A**) HEK293 cells were treated with either control, Sec62, or Sec63 siRNA for the indicated time points and analyzed by immunoblotting for the indicated antigens. IRE1α phosphorylation was probed by phos-tag-based immunoblotting. The percentage of IRE1α phosphorylation is shown underneath phos-tag immunoblots. (**B**) Wild type HEK293 or Sec63-/- cells were treated with 5μg/ml of Tm for the indicated time points and analyzed by immunoblotting for the indicated antigens. (**C**) Sec63-/- cells complemented with either WT or the J-domain mutant of IRE1α were treated with 5μg/ml of Tg for the indicated time points and analyzed by immunoblotting. The percentage of IRE1α phosphorylation is shown underneath phos-tag immunoblots. (**D**) HEK293 or Sec63-/- cells were transiently transfected with the indicated versions of Sec63 and treated with 5μg/ml of Tg for the indicated time points. The treated cells were directly harvested in SDS sample buffer and analyzed by immunoblotting for the indicated antigens. (**E**) Wild type HEK293 or Sec62-/- cells were treated with 5μg/ml of Tg for the indicated time points and analyzed by the immunoblotting for the indicated antigens.

Figure 3 – figure supplement 2. The effects of Sec63 depletion on activation of PERK and ATF6 during ER stress.

(**A**) The samples from Figure 3A were analyzed by immunoblotting for the indicated antigens. (**B**) The samples from Figure 3B were analyzed by immunoblotting for the indicated antigens. (**C**) HEK293 or Sec63-/- cells were treated with DTT for the indicated time points with the indicated concentrations. The cells were directly harvested in SDS sample buffer and analyzed by immunoblotting for the indicated antigens.

Figure 4. Biochemical reconstitution of Sec61/Sec63-mediated BiP binding to IRE1α.

(**A**) HEK293 cells were transiently transfected with either IRE1α-HA or its variants and immunoprecipitated using an anti-HA antibody and analyzed by immunoblotting. BiP binding to wild type IRE1α was set as 100%, and the percentage of BiP binding to IRE1α mutants were calculated with respect to wild type IRE1α. (**B**) HEK293 IRE1α-/- cells stably expressing IRE1α-HA or IRE1α-CNX-TMD-HA were treated with DMSO for 2h, 4mM DTT for 2h, 10μg/ml Tg for 2h, or 5μg/ml TM for 4h. The treated cells were harvested and analyzed as in A. The amount of Sec63 bound to wild type IRE1α from DMSO treated sample was set as 100%. The percentage of Sec63 bound IRE1α upon DTT, Tg, or Tm treated sample was calculated with respect to wild type IRE1α treated with DMSO. (**C**) A coomassie blue stained gel showing the purified IRE1α/Sec61/Sec63 complex or IRE1αΔ10 from HEK293 cells stably expressing either 2xStrep-IRE1α-FLAG or 2xStrep-IRE1α Δ10-FLAG. (**D**) A coomassie blue stained gel showing purified His-BiP from E. coli. (**E**) The purified IRE1α/Sec61/Sec63 complex, IRE1αΔ10 was bound to anti-FLAG beads and incubated with or without BiP in the presence or absence of ATP as shown. After incubation, IRE1α bound anti-FLAG beads were washed, eluted with sample buffer. A negative control reaction was performed by incubating empty anti-FLAG beads with the buffer, BiP, and ATP. The samples were analyzed by immunoblotting for the indicated antigens. BiP bands were quantified and presented as arbitrary units (a.u) after subtracting the buffer background.

Figure 4 – figure supplement 1. Sec61/Sec63-mediated BiP binding to IRE1α.
(**A, B**) HEK293 Sec63-/- cells complemented with wild type Sec63 were transiently transfected with either IRE1α-HA or its variants. The cell lysates were prepared either using the buffer containing NP40/deoxycholate or digitonin, followed by immunoprecipitation with an anti-HA antibody and analyzed by immunoblotting for the indicated antigens. (**C**) HEK293 cells were co-transfected with IRE1α-HA and empty vector or Sec63-FLAG or J-domain mutant of Sec63-FLAG. The cell lysates were immunoprecipitated with an anti-HA antibody and analyzed by immunoblotting for the indicated antigens. The amount of BiP binding to IRE1α that was co-transfected with empty vector was taken as 100%. (**D**) The purified IRE1α/Sec61/Sec63 complex or IRE1αΔ10 was incubated with or without BiP in the presence ATP. After incubation, IRE1α was immunoprecipitated using anti-FLAG beads. A negative control reaction was performed by mixing the buffer, BiP, and ATP, followed by immunoprecipitation with anti-FLAG beads. The samples were analyzed by immunoblotting for the indicated antigens. Note that IRE1αΔ10 contains a residual amount of the Sec61 translocon (long exposure blot), suggesting that weak binding between BiP and IRE1α Δ10 may be due to the presence of a small amount of Sec61/Sec63 in the sample. BiP bands were quantified and presented as arbitrary units (a.u) after subtracting the buffer background.

Figure 5. A model of the Sec61/Sec63/BiP complex-mediated regulation of IRE1α signaling.
(**A**) Step 1: The Sec61 translocon-associated Sec63 recruits and activates BiP ATPase via its luminal J-domain to bind onto IRE1α, thus preventing inappropriate activation of IRE1α under homeostatic conditions. Step 2: Upon ER stress, IRE1α is oligomerized and activated because Sec63 cannot efficiently recruit BiP, which is sequestered by misfolded proteins. The activated IRE1α mediates the splicing of the XBP1u mRNA that is bound to the Sec61 translocon through

its ribosome-nascent chain. Step 3: During prolonged ER stress, the level of BiP is significantly increased in the ER lumen. Hence, Sec63 can efficiently recruit and activate BiP to bind onto IRE1α to inhibit the oligomerization and activity of IRE1α. (**B**) Step 1: IRE1α can be partially activated if it either fails to interact with the Sec61/Sec63 complex or in Sec63 depleted cells. Step 2: Upon ER stress, IRE1α quickly forms higher-order oligomers or clusters, leading to hyper activation of IRE1α. Step 3: During prolonged ER stress, BiP cannot be efficiently recruited to inhibit IRE1α higher-order oligomerization in the absence of Sec63 despite the presence of excess BiP in the ER lumen. This leads to a severe defect in attenuation of IRE1α during persistent ER stress.

Li et al., Figure 1

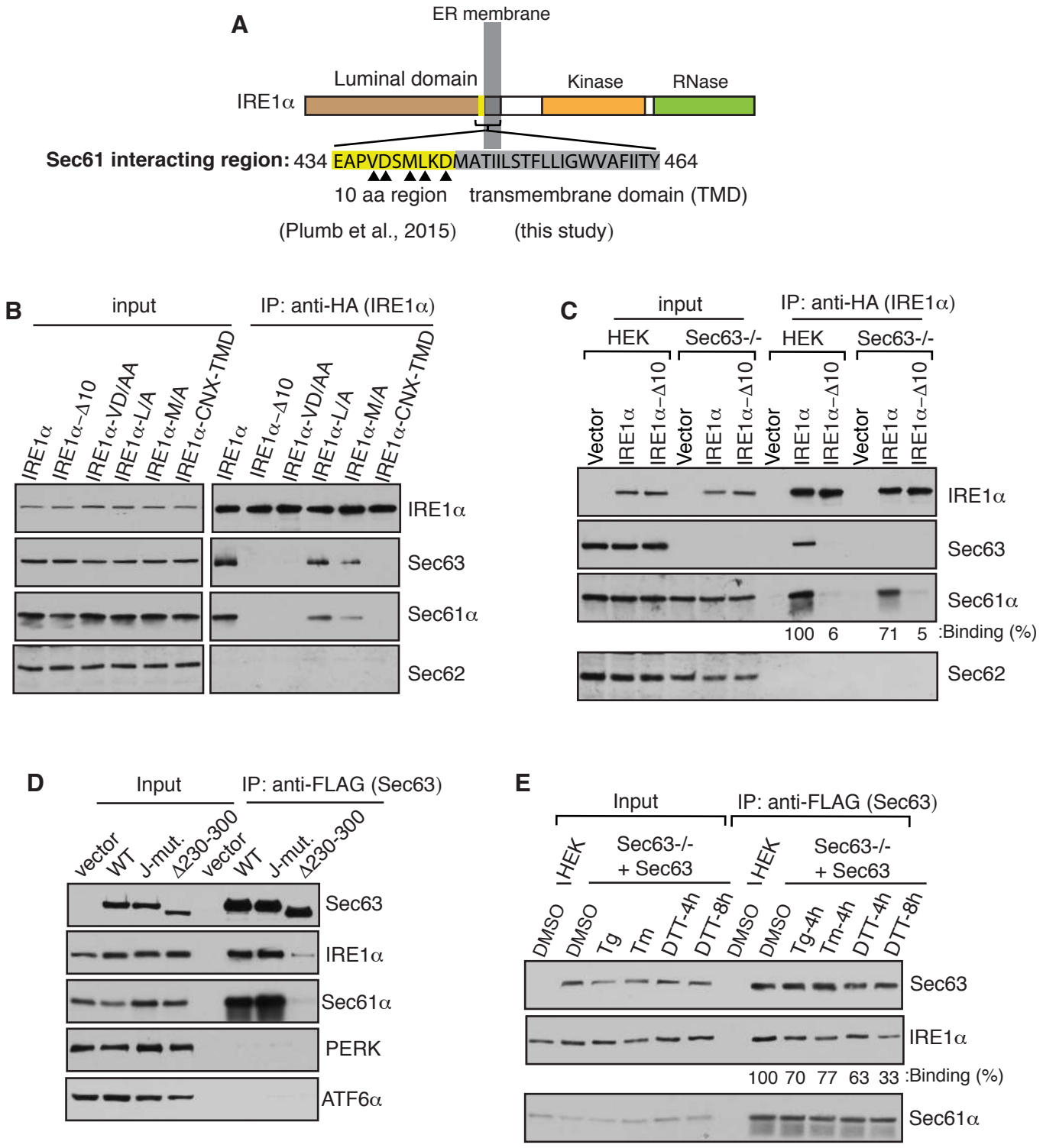

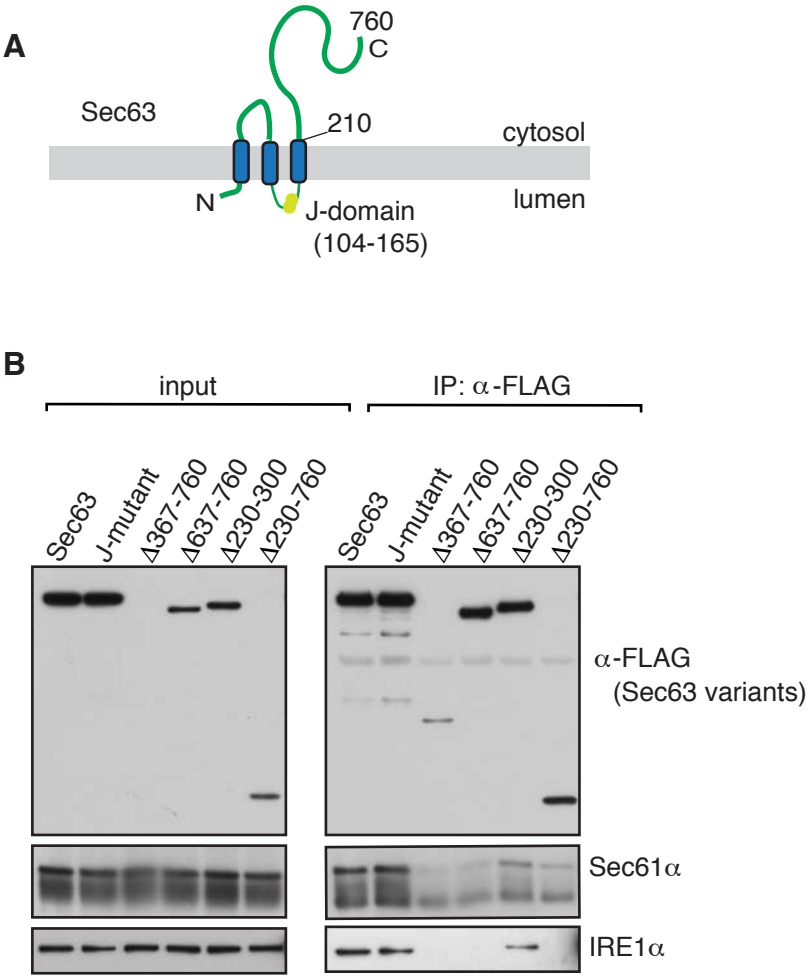

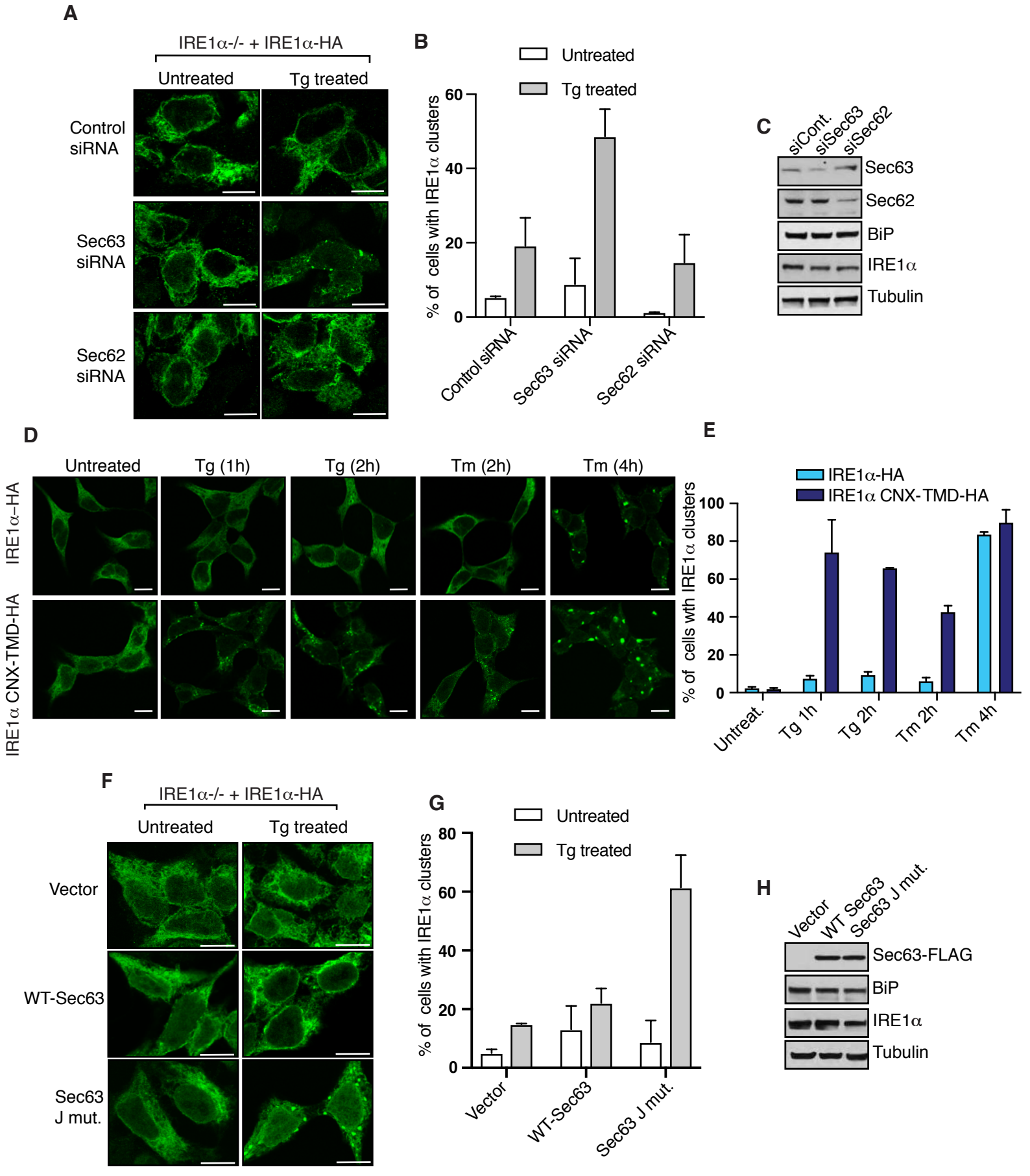

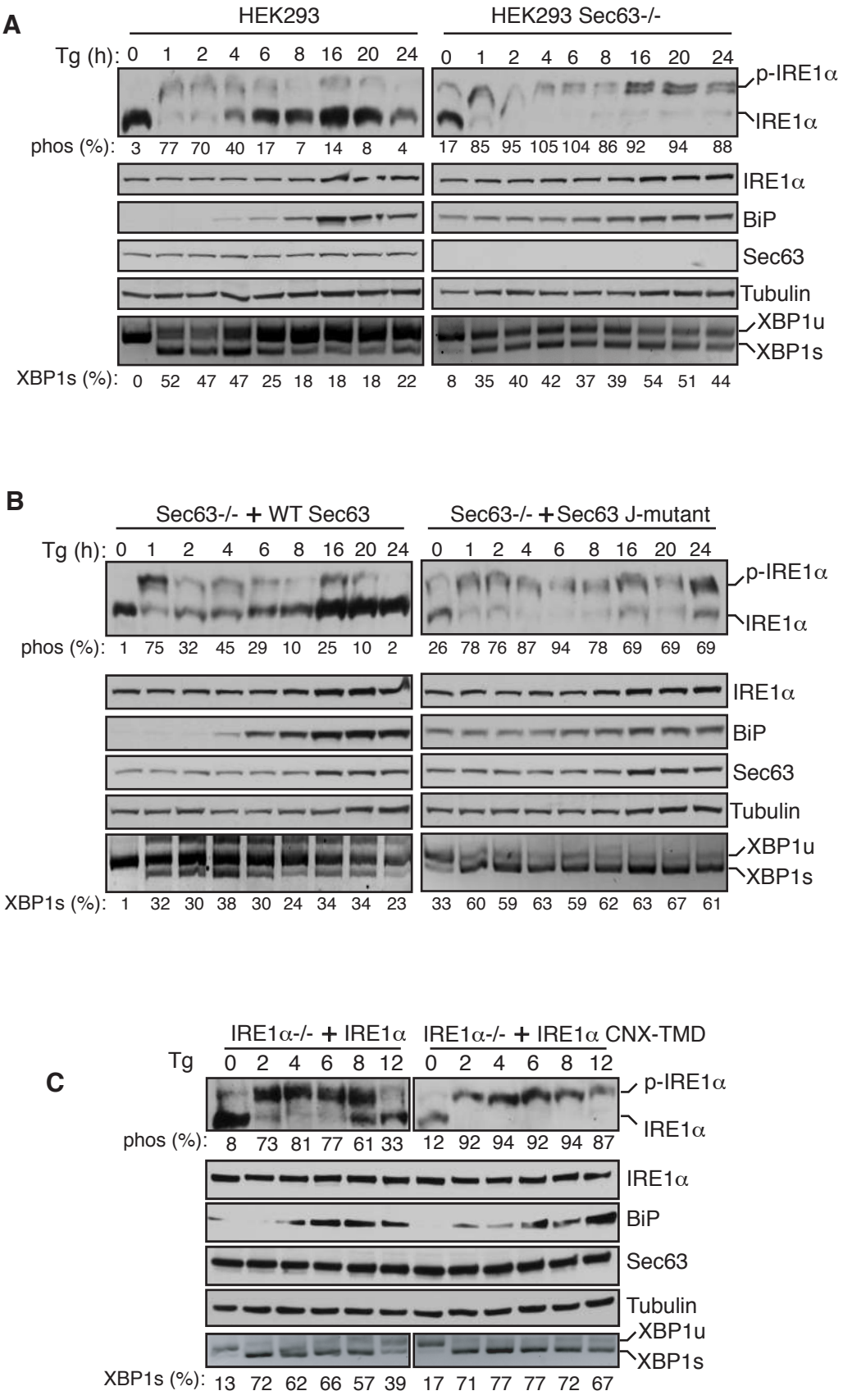

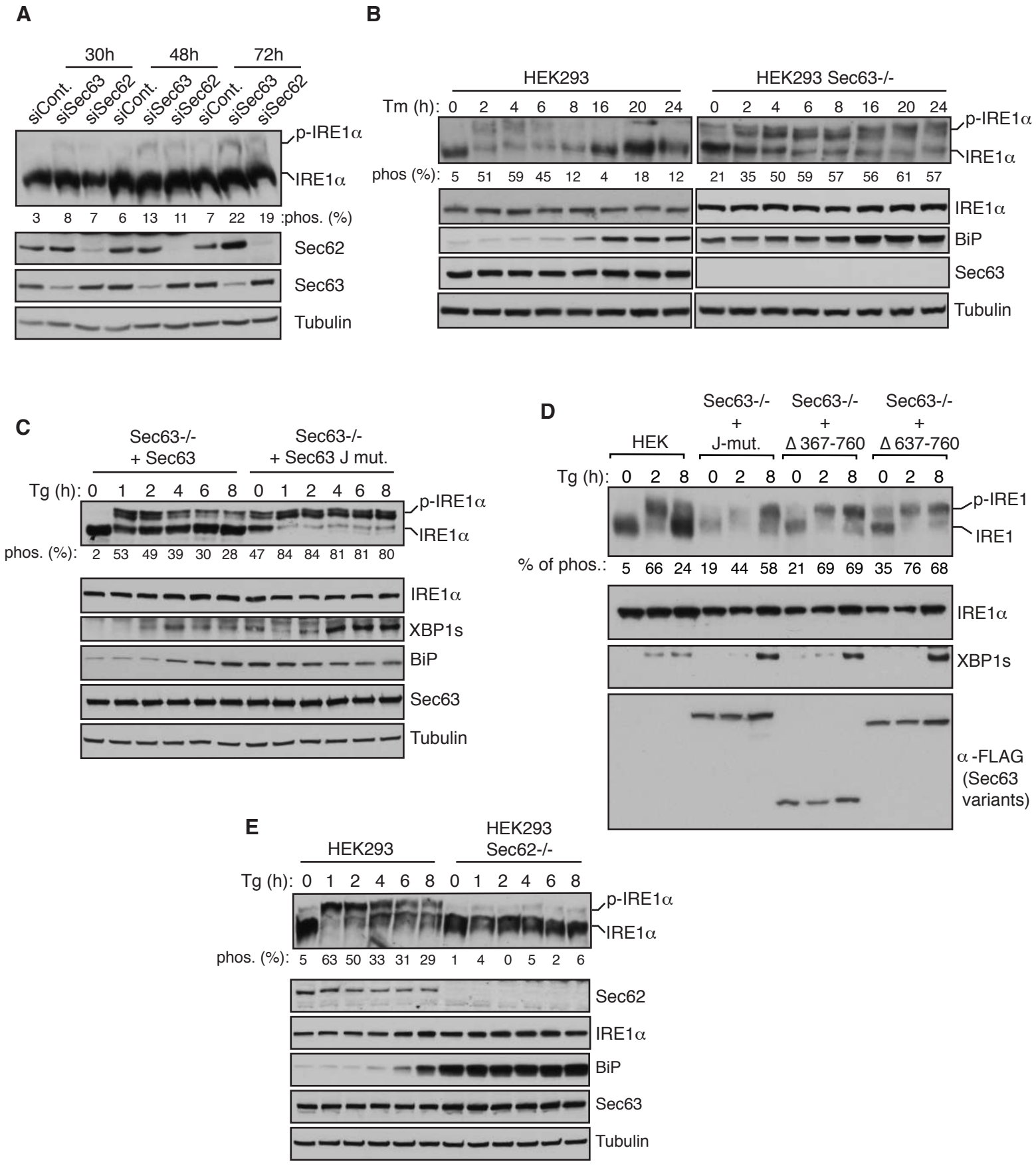

Li et al., Figure 3 – figure supplement 2

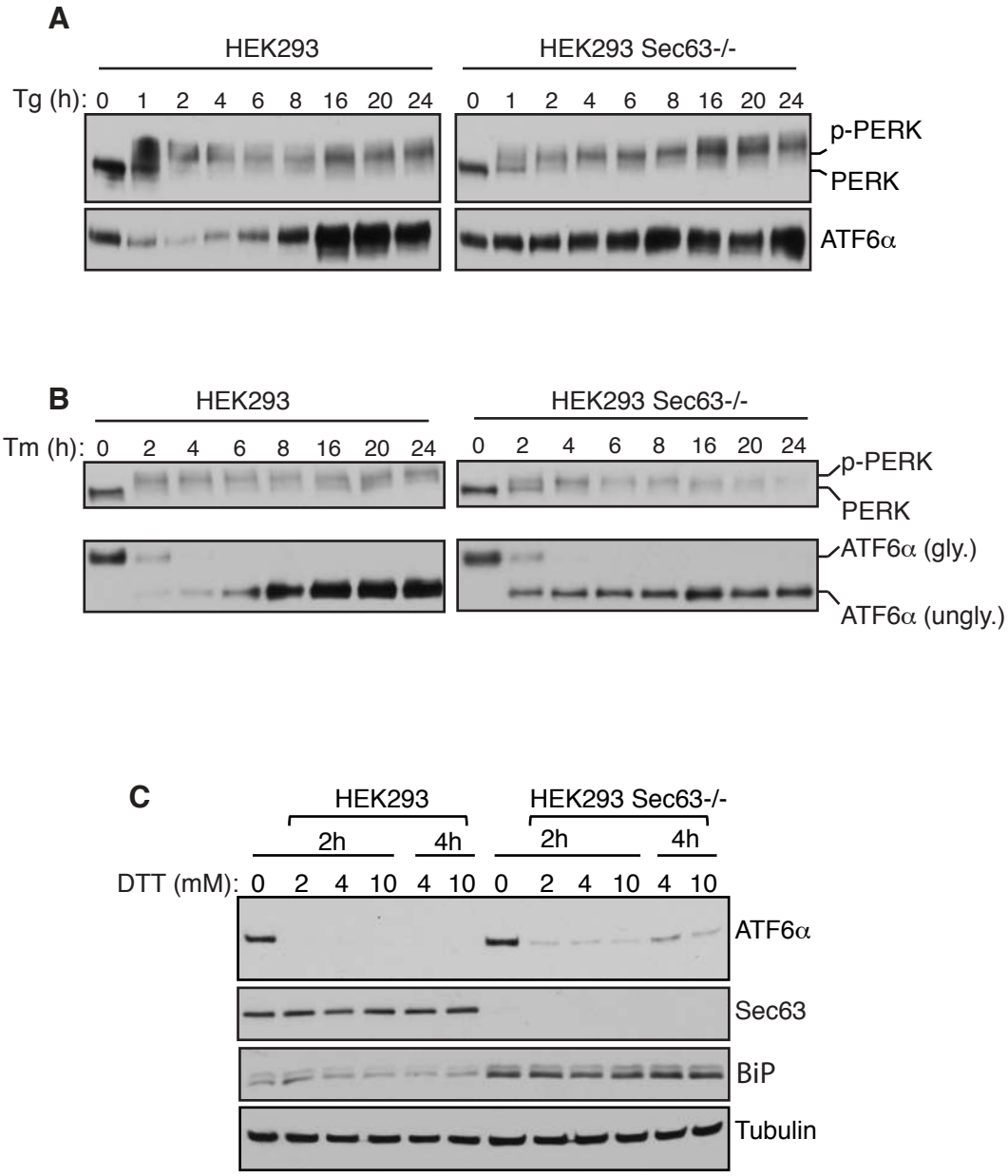

Li et al., Figure 4

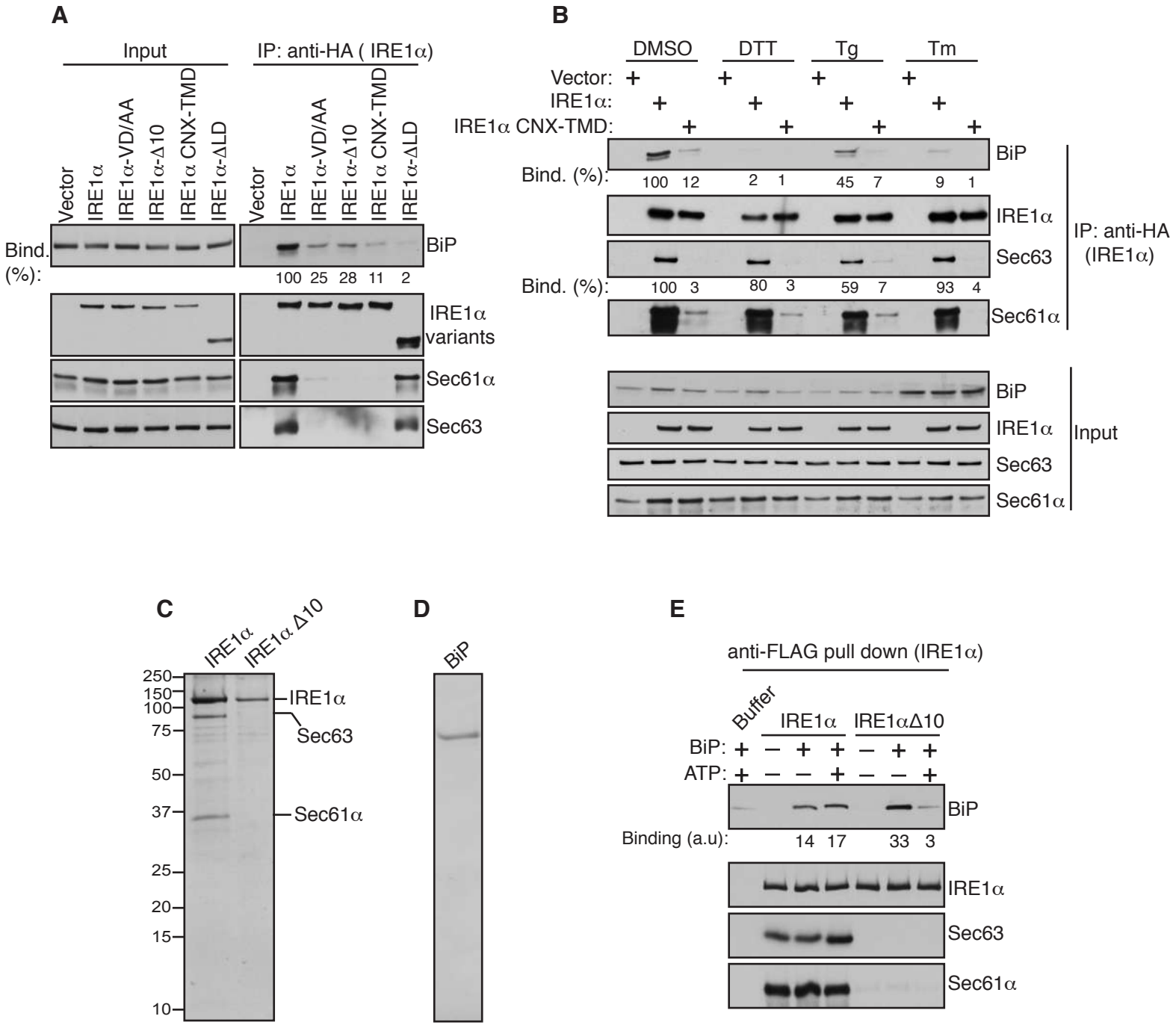

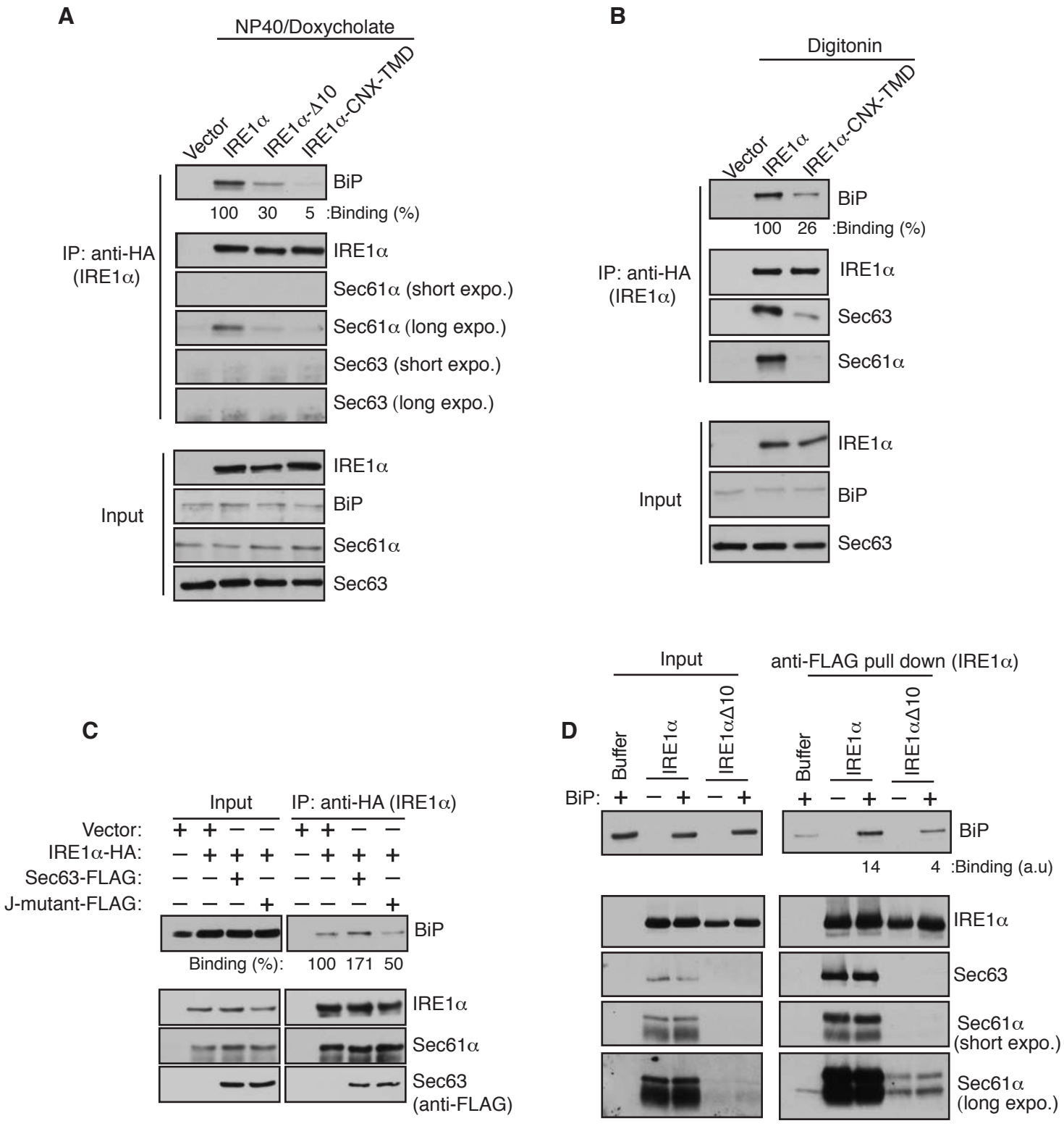

Li et al., Figure 5